Polypyrrole-Polyurethane based stretchable conductive composites using oxidative chemical vapour deposition

Chemical Engineering Master Thesis

Author: Mart Hendriksen

Student number: s3856852

University of Groningen

Faculty of Science and engineering

Date: 5-7-2021

First supervisor: Dr R. K. Bose

Second supervisor: Prof Dr F. Picchioni

ABSTRACT

Stretchable and flexible conductors have emerged as a cutting edge technology in the field of electronics. The combination of properties has led to new possibilities in intelligent, wearable and integrated systems. This work focuses on synthesising a Polypyrrole/Polyurethane (PPy/PU) based stretchable conductor in a heterogenous assembly design using oxidative chemical vapour deposition (oCVD). This research explores the effect of coating thickness and oCVD reaction temperature on the electromechanical behaviour of the stretchable conductor. Substrates from a selected PU grade were coated with PPy at three different reaction temperatures characterised by tensile test, Fourier transform infrared spectroscopy, differential scanning calorimetry, and dynamic mechanical analysis, followed by tests on conductivity piezoresistivity and durability. When the coating thickness became too high, the conductivity decreased, and the coating suffered from local fracturing under strain. However, when coatings were too thin, the conductivity decreased, and the samples showed piezoresistivity over a limited stretching range. TPU substrates that were coated at lower temperatures had generally a thicker coating, higher conductivity and showed piezo resistivity within a wide stretching range. At higher temperatures, however, the coating thickness, conductivity and range of piezoresistivity decreased. Durability tests revealed that the coated substrates did not recover conductivity after multiple stretching cycles, meaning that more research is required to make the stretchable conductor of interest to applications in stretchable electronics.

ACKNOWLEDGEMENT

At the times of planning, executing and evaluating the experimental work and writing this thesis, I was assisted by some great colleagues and supervisors. At this moment, I want to take a chance and thank them for their support and availability. Among a department full of friendly and helpful staff and students, I want to thank four people personally. First of all, thanks to Adrivit Mukherjee for sharing his vision on my project and helping me with designing some experimental methods. Secondly, I want to thank Dr Ranjita K. Bose for being my first supervisor who was available to share her knowledge in this field of research. Thirdly, I want to thank Prof. Dr Francesco Picchioni for being my second supervisor. And finally, thanks to Afshin Dianatdar for being a lab supervisor open for discussion, giving good suggestions and always supported me during this thesis. This work would not be possible without this incredible support.

ABBREVIATIONS

CNT: Carbon nanotubes

CP: Conductive polymer

CVD: Chemical vapour deposition

DMA: Dynamic mechanical analysis

DSC: Differential scanning calorimetry

FTIR: Fourier-transform Infrared Spectroscopy

oCVD: oxidative chemical vapour deposition

PDMS: polydimethylsiloxane

PPy: Polypyrrole

PU: Polyurethane

R: Resistance

SC: Stretchable conductor

T_g: Glass transition temperature

TPU: Thermoplastic polyurethane

CONTENTS

1 INTRODUCTION

In recent decades, few technologies have influenced our daily lives as electronics have. While the development of microchips mainly drives the electronic sector, new research fields have emerged, representing leading-edge technologies in electronics.[1] One of these technologies is flexible and stretchable electronics, which show exclusive properties. Therefore, it can offer new possibilities in innovative fields for intelligent, wearable and integrated systems. As a result, new applications come of interest, opening new markets including, but not limited to, healthcare, military and energy purposes.[2]

1.1 APPLICATIONS

In healthcare, several devices measure health-related parameters like heart rate and blood pressure, coming from multiple organs in the body. The skin is the largest organ of the human body and serves as a barrier to keep necessary chemicals in and infections out. Besides its numerous other functions to the main body, the skin's health-related signals from the inner organs are not always fully utilised. Stretchable electronics in wearable devices can serve as a new technology to serve as continuous health monitoring. In this application, the main challenge remains the different physical properties between stretchable electronics and the skin.[3]

The applications in wearable electronics are not limited to healthcare only. While this continuous monitoring could be used to measure health-related parameters, it can also pick up signals from the environment, which is a valuable feature for military applications. When on duty, soldiers must be equipped with technologies that improve communication, control and awareness. Wearable electronics can accommodate this by enhancing their mobility and energy efficiency.[4] However, a challenge in this field of application is that the materials require military-grade since they must sustain harsh conditions.[5]

Stretchable and flexible electronics can also contribute to the energy sector, both for harvesting as storage. In today's society, where the transition towards cleaner energy becomes more important, significant developments are still required. So far, strenuous efforts have been made to develop techniques to harvest energy to power electric devices. In particular, the harvest of mechanical and thermoelectrical energy is suitable to integrate into wearable devices as the device can be attached to the human body, which is often in motion and radiates heat.[6] This recollected energy must, of course, be stored as well.[7] However, while several stretchable sensors and electrodes become more available, designing stretchable energy-storing devices with the desired mechanical properties remains challenging.[2]

To summarise, there is a high demand for stretchable wearable electronics in several fields. This demand has led the scientific community to develop different design methods to accommodate the specifications of wearable electronics.

1.2 DESIGN

Generally, there are two methodologies to make stretchable electronic films. The conductive and stretchable components can be either mixed by homogeneous dispersion and heterogeneous assembly. Stretchable electronics produced by homogeneous dispersion consist of evenly distributed conductive nanoparticles in a polymer matrix. Within certain limits, the conductivity is tunable by the concentration of conductive particles in the matrix. If the concentration is too low, the conductive particles do not generate the pathway through the material for electrons to pass. On the other hand, when the concentration is too high, the filler aggregates, resulting in a decreased stretchability.[8] This method is usually chosen when the conductivity is expected from the bulk of the material.

On the other hand, Heterogeneous assembly is a method where the conductive layer is coated on the stretchable substrate. The main advantage of this design is a broader range of suitable conductive and stretchable materials. The stretchable substrate supports the conductive layer against excessive deformation. Both technologies have shown great potential and are therefore still widely researched. This work focuses mainly on the heterogeneous assembly method because of its wide range of suitable materials and the simplicity of the design. The following part elaborates on the type of suitable materials for stretchable conductors (SCs).

1.3 MATERIALS

SCs consist mainly of stretchable and conductive components. While the conductive fillers primarily determine the electrical properties of the SC, the mechanical properties are mainly controlled by the stretchable elastomeric matrix. Here, the intrinsic properties of the elastomer and the interaction between the conductive material and the elastomer govern the mechanical behaviour of the SC.

1.3.1 Stretchable substrates

Thus far, several materials have been reported to be suitable candidates to serve as a stretchable substrate. The most widely researched are natural rubber, styrene-butadiene rubber, ethylene-propylene-diene monomer, polyurethane (PU), thermoplastic polyurethane (TPU) and polydimethylsiloxane (PDMS).[8,9] Some of these materials have been reported with a reversible deformation of more than 200%. Therefore, they can support the conductive components by dispersing the stress over the matrix within an extensive stretching range.

For this research, the selected stretchable layer is PU, one of the most popular families of polymers due to its wide range of chemical structures resulting in versatile properties. Therefore, PU can be found everywhere in our daily life. The name is derived from the -NHCOO- bond, also called urethane, along the backbone chain (Figure 1). While these links are the most reactive parts of the molecule, it also contains other reactive functionalities which give polyurethanes general high compatibility with other polymers.[10] The urethane bond is formed with the reaction of two monomers: polyols and isocyanates. The large variety of these two monomers leaves possibilities for different PU structures and properties.[10,11]

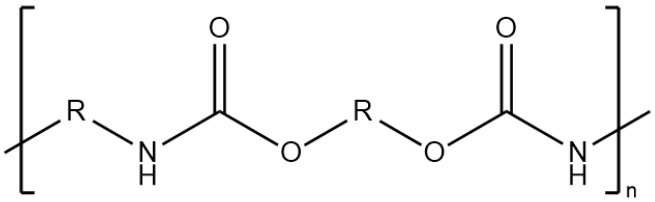

Figure 1: Structure of polyurethane

Among these different variations, thermoplastic PU (TPU) is the most popular due to its tuneability. In other words, the synthesis can be done according to the desired properties.[10] Diving into the macrostructure of TPU, it shows hard and soft segments (Figure 2). The soft segments consist of mostly polyols and serve the lower temperature properties like solvent resistance, weatherability and prevention against the agglomeration of hard segments. The hard segments are made from diisocyanates which form a rigid and crystalised segment in the macrostructure. These segments give the material more hardness and resistance against higher temperatures.[26] The combination of these segments provides the material with an elastic behaviour. On top of that, TPU is generally skin-friendly and biocompatible and is therefore frequently used in medical applications.[12] Combined with good stretchability and flexibility, it makes a good candidate for wearable electronic devices.

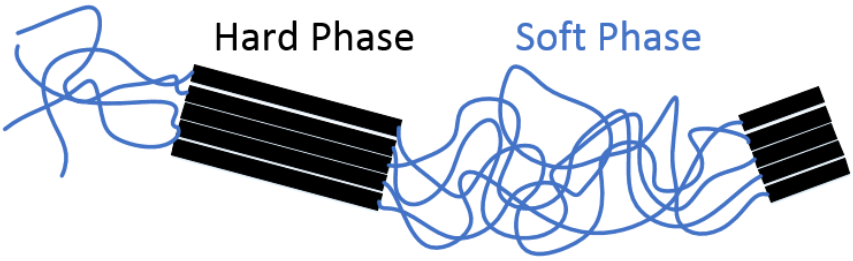

Figure 2: Hard and soft segments in the polyurethane macrostructure

1.3.2 Conductive fillers

The following part elaborates on the most researched conductive fillers, categorised into carbon-based, metal-based, or conductive polymers (CPs). This section discusses their merits and challenges, which are summarised in table 1.

Carbon-based materials have the advantage of good mechanical and electrical properties combined with cost-effectiveness. Among many different carbon-based material variations, carbon nanotubes (CNTs) are among the most promising.[13] Their high elasticity, thermal conductivity, low density and chemical inertness are features that led to a significant role in electronics.[14] Research by Sekitani et al. introduced the performance of CNTs, blended in an elastomer matrix. They synthesised an SC based on single-walled nanotubes dispersed over a fluorinated copolymer. The SC showed a conductivity of 57 S/cm unstrained and retained its conductivity till 6 S/cm when stretched upon 134% strain.[15] A more recent study by Wang et al. demonstrated an SC based on double-walled CNTs on a PDMS substrate. This SC showed a conductivity of 3316 S/cm when exposed to 100% strain.[16] The development of carbon-based SCs continues to improve its performance even further. The main challenges include inferior properties of the bulk produced CNTs, expensive scaling when used in composites and uncertainty about toxicity.[17]

Another popular material for stretchable electronics is metals. The outstanding conductivity over other materials has led to strenuous efforts to transform them into stretchable electronics. As the filler shape influences the mechanical and electrical properties of the device, metal fillers are used in different forms like nanoparticles, wires, sheets or flakes.[13] These shapes can be dispersed in a stretchable matrix or coated on a stretchable substrate to create a conductive pathway through the material. The good intrinsic conductivity and aligning behaviour of the nanoparticles result in outstanding performance when the SC is exposed to strain. While several shapes are used, nanowires often show the best performance. For example, in research by Lee et al., an SC was constructed of nanowires in a PDMS matrix. The conductor was able to stretch up to 460% without a significant decrease of conductivity.[18] While metal-based stretchable conductors have been reported as suitable candidates, their current limitation is the stability against oxidation which lowers the conductivity over time.

CPs have the advantage of tunable properties, good mechanical properties, easy synthesis and environmental stability.[19] The most common types are polypyrrole (PPy), Polyaniline, polyindiole and polythiophene. However, a current limitation is the poor solubility of these polymers, making them difficult to process. However, some efforts have been made to increase the solubility of the CPs. In research by Kayser et al., a more soluble poly(3,4-ethylene dioxythiophene): Polystyrene sulfonate (PEDOT: PSS) coblockpolymer was synthesised. Here the PEDOT is positively charged, and PSS negatively charged, making them dispersible in water. The material reached a conductivity above 1000 S cm^-1; however, it had a stretchability until 10% strain.[20]

Table 1: Conductive fillers with their merits and limitations

Conductive filler	Merits	Limitations
Carbon-based	high elasticity, thermal conductivity, low density and chemical inertness	Inferior quality in bulk, expensive scaling, uncertainty about toxicity
Metal-based	Very high conductivity, aligning behaviour of nanoparticles	Stability against oxidation
Polymer-based	Tunable properties, good mechanical properties, easy synthesis, environmental stability	Solubility issues, lower conductivity

While all types of materials have particular merits, this work narrows down to CP based SCs. The selected conductive coating is Polypyrrole (PPy). PPy is the most researched CP because of its straightforward synthesis, good conductivity, high stability and good redox properties.[21] Regarding pyrrole structure, the nitrogen atom in the conjugated ring opens possibilities for different reactions [22], including oxidative polymerisation. In this mechanism, an oxidant removes an electron from the pyrrole molecule, followed by dimerisation of two pyrrole molecules. After deprotonation, a stable dimer is formed, reacting again with the oxidiser. This type of reaction is called step-growth polymerization (Figure 3).[23]

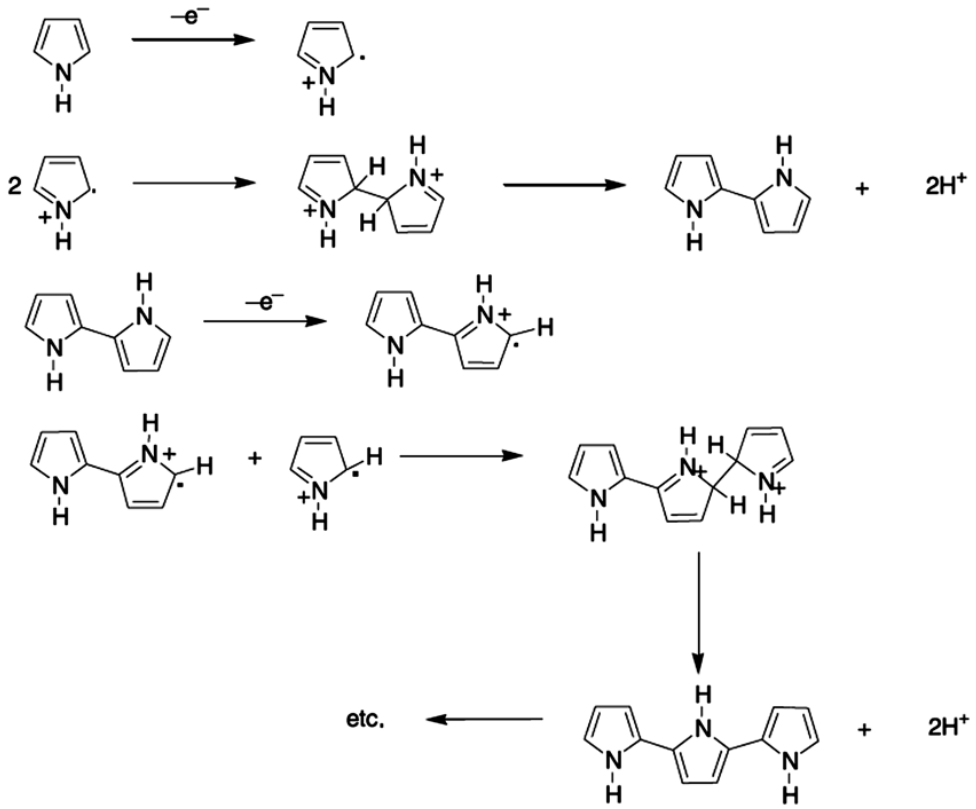

Figure 3: oxidative polymerisation of PPy [23]

The PPy structure shows that the backbone chain is conjugated.[24] This characteristic can be exploited by making deliberate imperfections in the structure of the chain. This is called the doping process. The dopant is added to the conjugated polymer and acts as an electron acceptor. By partially oxidising the polymer chain, a cation is formed. Hence an electron is missing in the structure.[25] The missing charge is compensated by an anion, making PPy an organic salt after the doping procedure. The doping process increases the electron mobility and transforms the originally insulating PPy into a semiconductor.

In order to make the two selected materials function as a stretchable conductor, several fabrication techniques have been developed. The following part gives an overview of the common techniques and compares them to each other.

1.4 FABRICATION

Different methods are suitable for assembling the stretchable and conductive layers, each having its benefits and limitations. They can be divided into wet processing and dry processing.[2]

Wet processing mainly includes drop casting, spin coating, dip coating, doctor blading and spray coating.[2] The drop-casting method is the most straightforward as it involves casting a solution on a substrate followed by solvent evaporation (Figure 4A). While this method does not waste any material, it faces non-uniformity and non-controllable film thickness at large scale operations.[26] In spin coating, a solution is cast on a rotating plate (Figure 4B). This method has better controllability on film thickness and gives more uniformity. Still, there is a waste of material, and the procedure does not work for large areas. In addition, the solvent evaporates fast, preventing a controlled molecular ordering which influences the crystallinity of the coating.[26] Doctor blading involves casting a solution on the substrate followed by a constant, controlled parallel movement of a blade (Figure 4C). This procedure generates a uniform film with controllable thickness without having any waste of material. However, the challenge is to regulate the micrometric precision of the blade.[2] Dip coating is a technique where the substrate is immersed in the coating solution followed by withdrawal of the substrate (Figure 4D). The process can be controlled by factors like withdrawing speed, solvent volatility, viscosity and concentration of the liquid. Therefore, this process can make thin, uniform layers with the possibility to cover large areas. The drawbacks are the waste of material, a time-consuming process and coating on both sides of the substrate.[26] Spray coating uses an atomiser to spray the coating solution onto the substrate (Figure 4E). This technique can be applied to large areas, and the film thickness is well controlled. However, the downside is the homogeneity of the film, which is challenging to regulate.

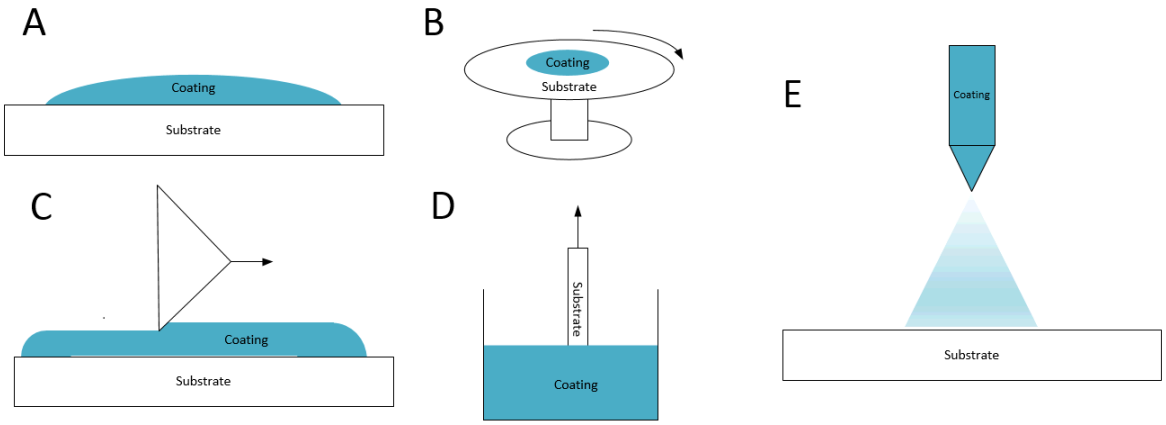

Figure 4: Wet processing. A: Drop casting, B: Spin coating, C: Doctor blading, D: Dip coating, E: Spray coating

While wet processing methods are widely used in research, they still face common challenges. Firstly, it encounters dissolution, mixing or cracking of the stretchable substrate.[27] Secondly, the dispersion of conductive material often faces wettability issues [26] and cannot distribute the coating in a non-planar 3D structure [28], resulting in non-uniform films. More uniformity would result in fewer defects and increased performance.[1,29] Dry processing could overcome these limitations.

Dry processing does not include solvents as it occurs in the vapour phase. The most researched variations are atomic layer deposition and chemical vapour deposition (CVD).[30] Atomic layer deposition is a reaction technique in a vacuum where the reactants are introduced to the reactor in purges. By introducing the reactants in sequence, the growth of the coated film can be controlled layer by layer. The film growth is limited to the reaction on the surface. In CVD, however, the reactants are introduced simultaneously into the reactor. Here, the reaction occurs both on the surface and in the gas phase, followed by deposition. Compared to atomic layer deposition, the CVD reactions often have a higher activation temperature. Therefore, different variations of CVD have been developed to stimulate the reaction. Some examples are the use of a filament wire (Initiated CVD), a plasma (Plasma enhanced CVD) or an oxidant (Oxidative CVD). While atomic layer deposition and CVD have particular merits, the techniques are relatively new and not thoroughly researched compared to wet processing techniques.

As a summary, table 2 compares both wet and dry processing methods. As highlighted in this paragraph, the fabrication techniques are numerous, and each has specific advantages. This work focuses on the use of CVD in the synthesis of a PPy/TPU based SC.

Table 2: Comparison of wet and dry coating methods [2,26–29]

Technique	Complexity	Waste of material	Controllable thickness	Uniformity	Area size	Dissolution issues	Substrate cracking	process speed
Drop casting	-	-	-	-	-	+	+	±
Spin coating	-	+	+	+	-	+	+	+
Doctor blading	±	-	+	+	+	+	+	±
Dip coating	±	+	+	+	+	+	+	-
Spray coating	±	-	+	-	+	+	+	±
Chemical vapour deposition	+	-	+	++	-	-	-	±
Atomic layer deposition	+	-	+	++	-	-	-	±

Many different types of CVD have been invented and investigated. Amongst these types, oxidative chemical vapour deposition (oCVD) is a suitable technique for synthesising conductive coatings.[31] Figure 5 depicts a schematic setup of the oCVD reactor.

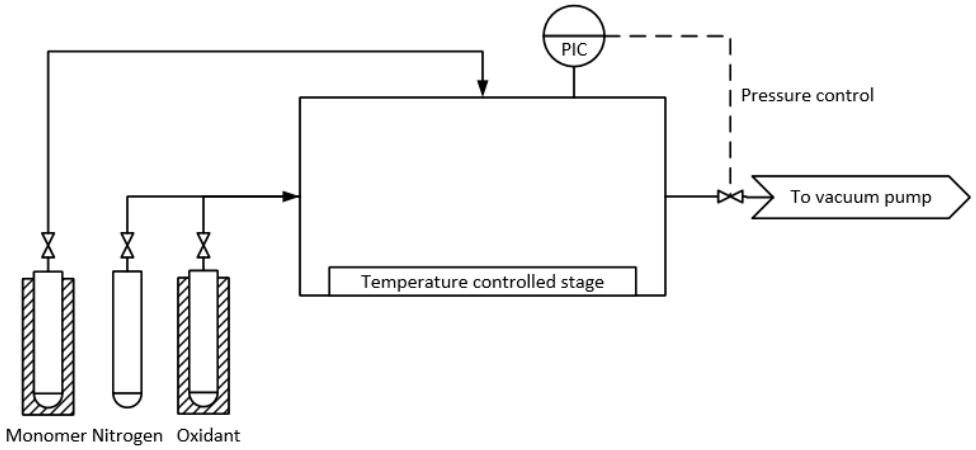

Figure 5: Schematic setup of the oCVD reactor

The pressure is a critical process variable as it controls the concentration of chemicals in the reactor and should be low enough to generate a vapour stream. Another crucial variable is the temperature, which is monitored at multiple locations in the system. The monomer and the oxidant containers are kept at elevated temperatures to increase vapour formation. The lines are heated up to prevent inline deposition, and the stage temperature is kept at relatively lower temperatures. This sudden decrease in temperature ensures the deposition on the stage. However, the stage temperature should not be too low since it also influences the reaction rate. At higher temperatures, however, it was found by Drewelow et al. that higher substrate temperature resulted in less adsorption to the surface. At this point, the reaction changes from kinetically limited to mass transfer limited, and the deposition rate decreases.[32] Finally, the ratio between monomer, oxidant, and nitrogen influence the reaction kinetics. Here, nitrogen acts as an inert carrier gas that supports the oxidant flow and partially controls the polymerisation reaction.[33] To summarise, the main controlling factors for the film growth are reactant ratio, reactor pressure, and substrate temperature—the precise control results in the synthesis of uniform and defect-free films.[31]

The use of oxidants is a critical factor for the reaction rate and the step-growth polymerisation mechanism. So far, both solid as liquid oxidants have been researched in the field of oCVD.[29] While liquid oxidants have not yet shown compatibility for all possible monomers, they offer multiple benefits over solid oxidants, which is why they are preferred in this work. For instance, the unreacted oxidant leaves the reactor, meaning no post-reaction rinsing step is required.[34,35] Moreover, the more volatile compounds have more sticking probability onto the substrate, resulting in more conform deposition.

oCVD has the potential to become a suitable fabrication technique for CP-based SCs. However, so far, the application to the field of stretchable electronics has not yet been thoroughly researched. Nevertheless, the hypothesis states that oCVD could add multiple benefits to the synthesis of SCs. Therefore, this work focuses on synthesising a CP-based SC through a heterogeneous assembly design using oCVD.

2 RESEARCH QUESTIONS AND HYPOTHESES

In this thesis, the SC is synthesised, characterised and tested on conductivity under deformation. The synthesis part focuses on the selection of the stretchable substrate and the optimisation of the oCVD reaction. After that, the SCs are characterised, followed by testing on electromechanical behaviour. In this research, the following questions are tried to be answered.

1. What TPU substrate is the most suitable based on mechanical behaviour, and what is the elastic region of this material?

As mentioned in the theory section, the stretchable layer is the fundament of the device. Therefore, the first part of the research is the analysis of the substrate. Here the mechanical properties of multiple TPU series are analysed. The substrate should not deform under stress during its practical use, so the elastic region should be determined.

2. How does coating thickness influence the electromechanical behaviour of the SC?

The thickness of both layers can influence mechanical properties as well as electrical performance. By a rule of thumb, the thicker and stiffer the deposited material and the thinner the stretchable substrate, the lower the intrinsic stretchable properties the device will have.[36] Regarding the electrical properties, the deposited layer must be thick enough to create a linking passage that can pass an electric current to be conductive. However, when the layer thickness is too large, the conductivity tends to decrease because of more defects.[37] Hence, the optimal layer thickness is not known and must be optimised with respect to the electromechanical performance of the SC.

3. How does reaction temperature influence the electromechanical behaviour of the SC?

In research by Dianatdar et al., the oCVD conditions like reactant ratio, reactant temperature, deposition pressure and substrate temperature for the PPy synthesis were optimised (This work has not yet been published). However, in this research, the temperature influences the stretchable substrate as well. As a result of an increased temperature, the polymer chains of TPU can move more freely in the macrostructure. Thus, at a higher temperature, more gas reactants can infuse into the structure, which can result in more incorporation of the PPy in the TPU substrate. Matsunaga et al. studied the permeability of gas into TPU.[38] It was found that at higher temperatures, the diffusion and permeability coefficients increase, corroborating the hypothesis.

3 EXPERIMENTAL

3.1 MATERIALS

The chemicals used for the oCVD reaction were pyrrole and antimony(V) pentachloride, both purchased from Sigma Aldrich. In this research, antimony pentachloride was selected because it is one of the few suitable liquid oxidants and was reported multiple times as an effective oxidant.[33,39,40] Table 3 shows the tested TPU series, including the company and state of delivery. As the table shows, the state of the materials varied. Hence, they needed different preparation methods to produce a thin film which are described in the following section.

Table 3: TPU series

Name	Company	State
Neorez R-1005	DSM	Water-based dispersion
Neorez R-1007	DSM	Water-based dispersion
Elastolan 1170 A10	BASF	Solid pellets
Elastolan 1185 A10	BASF	Solid pellets

3.2 SUBSTRATE PREPARATION & TENSILE TEST

The Neorez R-1005 and R-1007 substrates were prepared by casting the PU dispersions on a PTFE plate. The Elastolan 1170 A10 and 1185 A10 pellets were dissolved in THF (10 wt.%) and stirred for 2 hours at room temperature. Next, the solution was cast on a PTFE surface and carved with a film applicator (height of 2 mm), after which it was left to dry overnight at room temperature and atmospheric pressure. The films were covered with aluminium foil (with holes) to control the drying process and prevent contamination and bubble formation. The substrates (length: 18 mm, width: 6.2 mm, thickness: 0.12 mm) were tested by an INSTRON 5565 tensile tester with a 50 mm/min crosshead speed.

3.3 OCVD EXPERIMENTS

During the oCVD experiments, free-standing TPU films, glass slide and silicon wafer were placed in the deposition chamber (Figure 6), after which it was closed and put under vacuum. The experiment started after the base pressure and leak rate were below 90 mtorr and 0.15 sccm. The oxidant and monomers were preheated to 60°C, and the lines were heated to 110°C. The flow rate of the chemicals was calculated with the following formulas.

$$\frac{dn}{dt} = \frac{dp * V_{reactor}}{R * T * dt} \quad \left(\frac{mol}{\min}\right) \qquad (1)$$

$$\frac{dv}{dt} = \frac{\left(\frac{dn}{dt}\right) * R * T}{P} * 100^3 \quad (sccm) \qquad (2)$$

By measuring the pressure over time, the flow rate was calculated. The targeted flowrates for nitrogen, pyrrole and antimony (V) pentachloride were 2, 2,5 and 0,5 sccm, respectively. After calibration of the incoming flows, the valves were opened, and the reactor was set to the desired base pressure and temperature. After the reaction, the substrates were stored in an inert environment for analysis. oCVD was used three times at different conditions (Table 4). In the experiment with the highest temperature, the reaction time was increased to ensure measurable deposition of PPy coating.

Table 4: oCVD reaction conditions

Experiment	Temperature (°C)	Reaction time (min)
Temperature 1	40	30
Temperature 2	50	30
Temperature 3	60	40

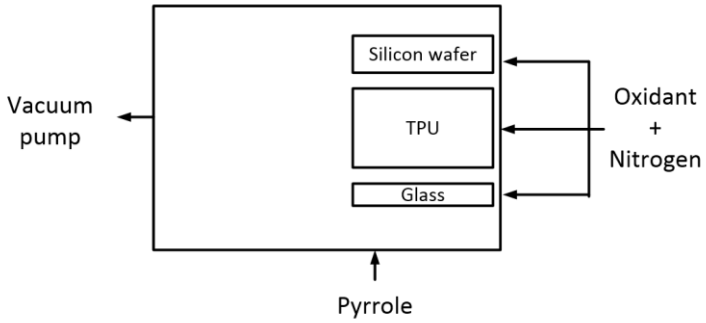

Figure 6: Top view oCVD reactor with substrate configuration

3.4 CHARACTERISATION

The Fourier transform infrared spectroscopy (FTIR) (Shimadzu IRTracer instrument) was operated in transmission mode with the following settings: Scans: 128, resolution: 8 cm^{-1}. The dynamical mechanical analysis (DMA) (DMA 8000 Pyris) was operated in tension mode with the following settings: Temperature range: -80 °C to 40°C, strain: 0.03 mm, frequency: 1 Hz. Differential scanning calorimetry (DSC) (TA Instruments DSC 25) was used with the following method: Temperature range: -90 to 100°C, heating rate: 10°C/min. The PPy coated TPU substrates (length: 18 mm, width: 6.2 mm, thickness: 0.12 mm) were tested by an INSTRON 5565 tensile tester with a 50 mm/min crosshead speed.

3.5 ELECTROMECHANICAL BEHAVIOUR

The electrical resistance was measured with a modular digital multimeter (Keysight Benchvue U2741A). Here two electrodes were attached to the sample followed by continuous resistance measurement. The conductivity was calculated by plugging in the measured resistance and the sample geometry in formulas 3 and 4.

$$\rho = R * \left(\frac{A}{L}\right) \quad (\Omega m) \qquad (3)$$

$$\sigma = \frac{1}{\rho} \quad \left(\frac{S}{m}\right) \qquad (4)$$

The piezoresistivity measurements were done with a rheometer (TA HR20) in tension mode. The samples were clamped in a rheometer while the clamps were wired to the electrodes for continuous resistance measurement. The sample (length: 15 mm, width: 6.2 mm, thickness: 0.12 mm) was stretched with a crosshead speed of 30 µm/s.

The durability (resistance after multiple stretching cycles) was continuously measured in the rheometer. In this procedure, the samples (length: 15 mm, width: 6.2 mm, thickness: 0.12 mm) were subjected to cyclic loading with continuous resistance measurement. The crosshead speed of the rheometer was 100 µm/s.

4 Results and Discussion

4.1 Substrate analysis

As part of the synthesis of the SC, the different TPU substrates were tested on stiffness and stretchability by tensile test and cyclic loading, respectively. From these tests, one type of TPU is selected to be most suitable for this research. In the following part, the test results are discussed.

The stress-strain graphs (appendix 1) show the intrinsic difference in behaviour between the Neorez series and Elastolan. In the first percentage of strain, the Neorez series showed an immediate increase in stress, followed by deformation. This behaviour indicates a small elastic region, so these series were discarded in the early stage. Figure 7 shows the tensile test results of the more suitable Elastolan series. Here, the stress at 20%, 100% and at the breaking point, as well as the elastic modulus, are given to indicate the stiffness of the material. The stress-strain graphs are displayed in appendix 2.

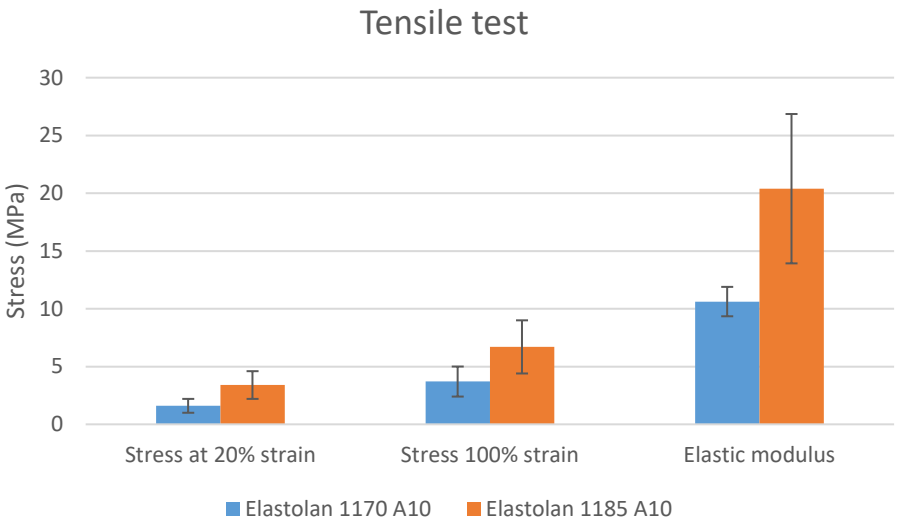

Figure 7: tensile test on Elastolan series

The tensile test indicates that Elastolan 1170 A10 has lower stress values at 20% and 100%. Besides, the elastic modulus of Elastolan 1170 A10 is significantly lower. Therefore, all measured values suggest that Elastolan 1170 A10 has a lower stiffness, making it the most suitable TPU grade among the four tested types. However, while the tensile tests were used to determine stiffness, it was impossible to decide on an elastic region. As shown in the stress-strain graphs in appendix 2, the point of deformation, where stress becomes lower with respect to the strain, has no apparent onset. Therefore, cyclic loading tests were used to determine the elastic portion of Elastolan 1170 A10.

The elastic region in the material is where the SC works in the application. Therefore, it is essential to determine which extend it can stretch before deformation. In the following tensile tests, the materials are subjected to cyclic loading. Herein the material was stretched to a predetermined strain, after which it returned to the original position (Figure 8). This procedure was repeated for five cycles to determine whether there is deformation or not.

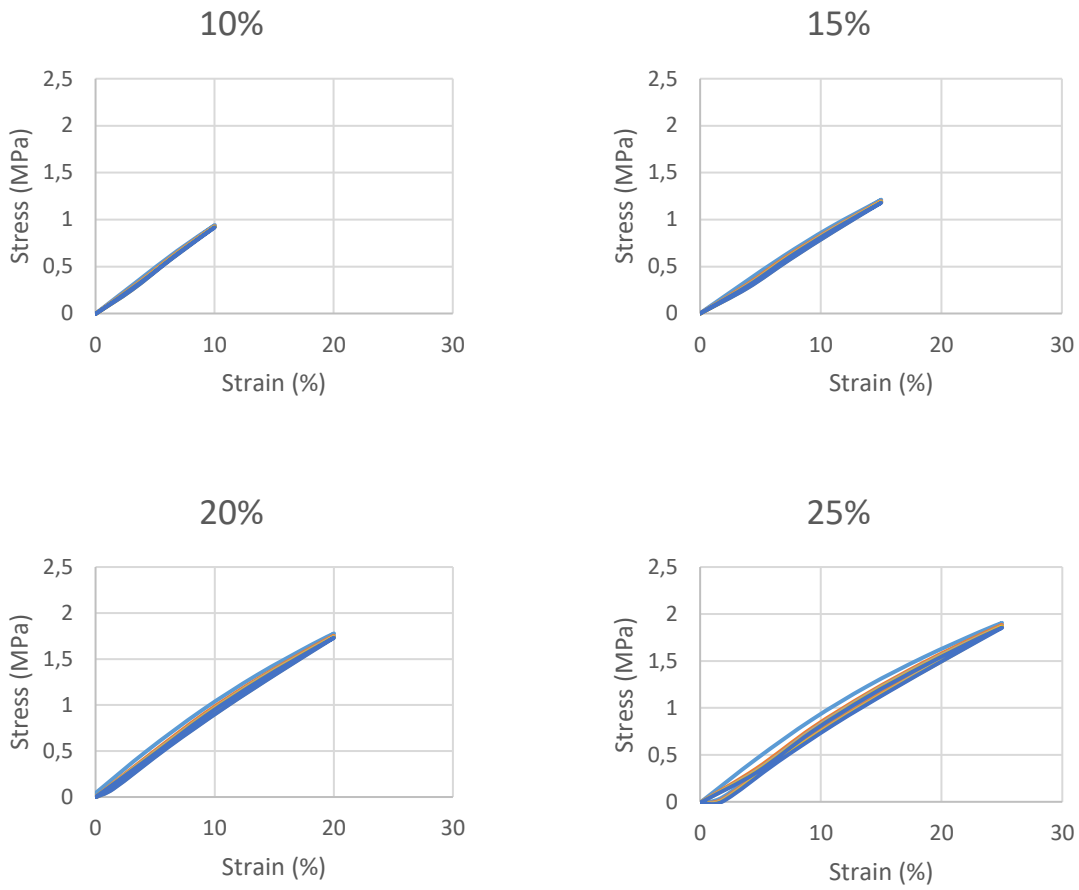

Figure 8: Cyclic loading test on Elastolan 1170A10

The graphs show a linear behaviour when approaching the 10%, 15 and 20% strain limit (Figure 8). The stress-strain graphs return to the original position in these graphs, indicating no plastic deformation in de consecutive cycles. However, the 25% strain cycles show that the stress decreases after multiple cycles, meaning the material passed the elastic region. The limit of the elastic region of Elastolan 1170 A10 is determined at 20%. In the following sections, Elastolan 1170 A10 is referred to as TPU.

4.2 CHARACTERISATION

The coated substrates were analysed with different methods to confirm and quantify PPy deposition onto the TPU substrate. The peaks at 1550, 1300, 1170, and 1050 cm^{-1} indicate the C=C, C-N, C-H, and C-C bonds (Figure 9). Regarding the PPy structure, the C=C, C-N and C-H bonds are present in the cyclic pyrrole structure, while the C-C bond indicates the link between the two pyrrole molecules. This link between the monomers represents a successful polymerisation.[41]

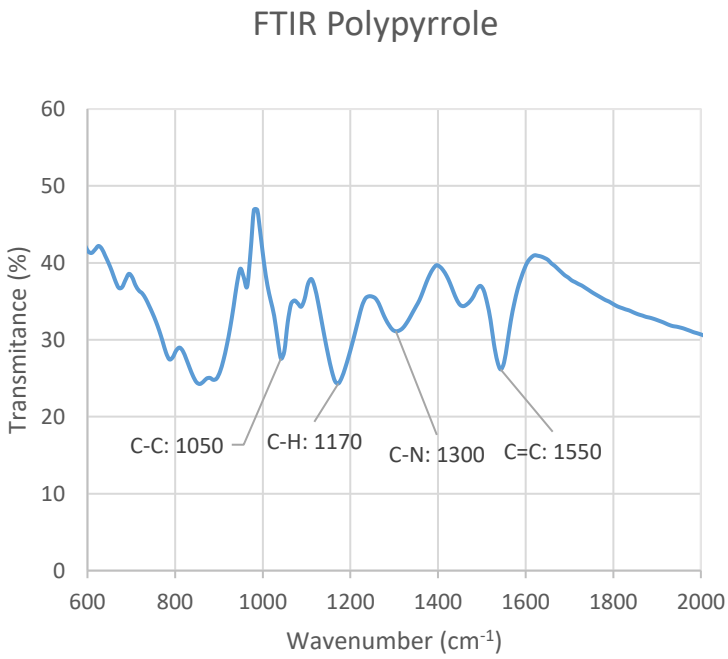

Figure 9: FTIR scan of PPy

The DSC analysis was used to determine the glass transition temperature (T_g) of the coated and uncoated substrate for comparison (Figure 10). Both samples pass the T_g within the temperature range, indicated by the sudden decrease in heat flow. The DSC scan suggests that the T_g of TPU increases when coated with PPy. Knowing that the phase transition from glass to rubbery state occurs when the hard segments in the polymer chains become mobile, it can be explained that this T_g shift is caused by the stiffer PPy, which is uniformly coated on and into the TPU substrate. As a result, the large segments require more energy to display chain mobility, causing the T_g to increase. The T_g shift was also observed in research on the properties of PPy/TPU composites by Yanilmaz et al. They explained this by the interaction of the two materials at the molecular level. It was suggested that the amide groups of PPy and the carbonyl groups of PU formed hydrogen bonds, which helped to improve their phase mixing.[42]

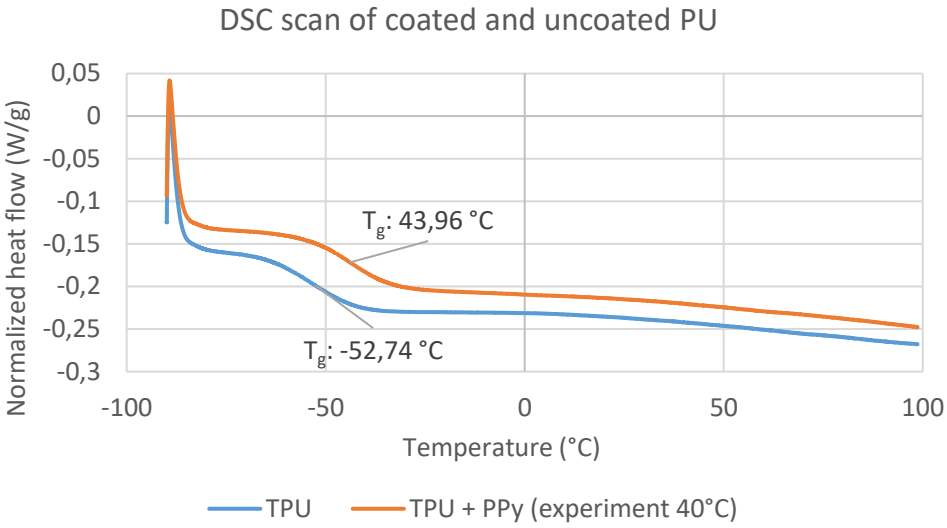

Figure 10: DSC scan of coated and uncoated TPU

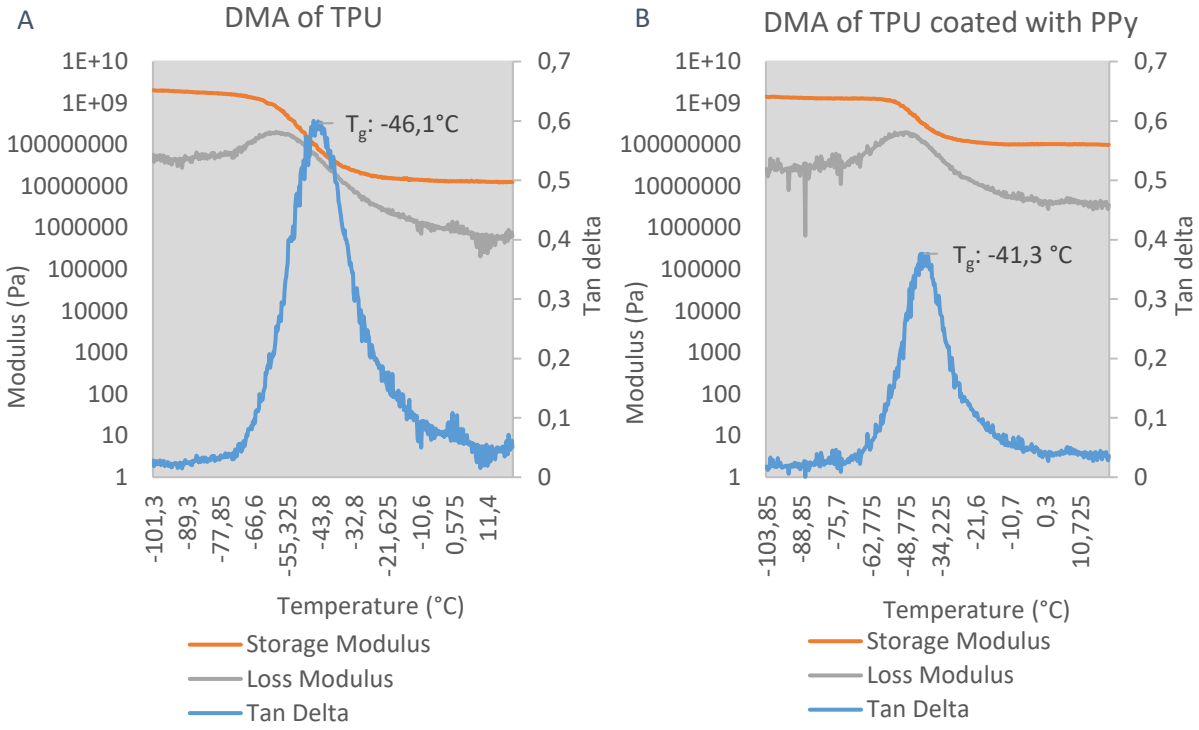

Figure 11: DMA of A) TPU and of B) TPU coated with PPy (experiment 40°C)

The DMA was used to determine the thermomechanical behaviour of the coated and uncoated substrate (Figure 11). The tan delta, indicating the ratio of the elastic response over the viscous response of the material, is significantly lower for the coated substrates. The lower storage modulus mainly causes the lower value for tan delta. This suggests that the elastic response is compromised by the PPy coating[43], which can be explained by the stiff mechanical behaviour of PPy.[44] Comparing the tan delta peak, which indicates the glass transition, the graphs show that the coated sample has a higher glass transition. This observation agrees with the T_g shift noticed in the DSC measurements (Figure 10).

With profilometry, the coating thickness as a function of the distance from the inlet was determined (Figure 12). The graphs show that the deposition decreases with higher reaction temperature, suggesting that the oCVD reaction kinetics are mass transfer controlled. This was also found in the oCVD experiments by Drewelow et al., where the deposition rate of PEDOT decreased with increasing substrate temperature.[32] They explained this by the higher vapour pressure at higher temperatures, lowering the absorption rate on the substrate.

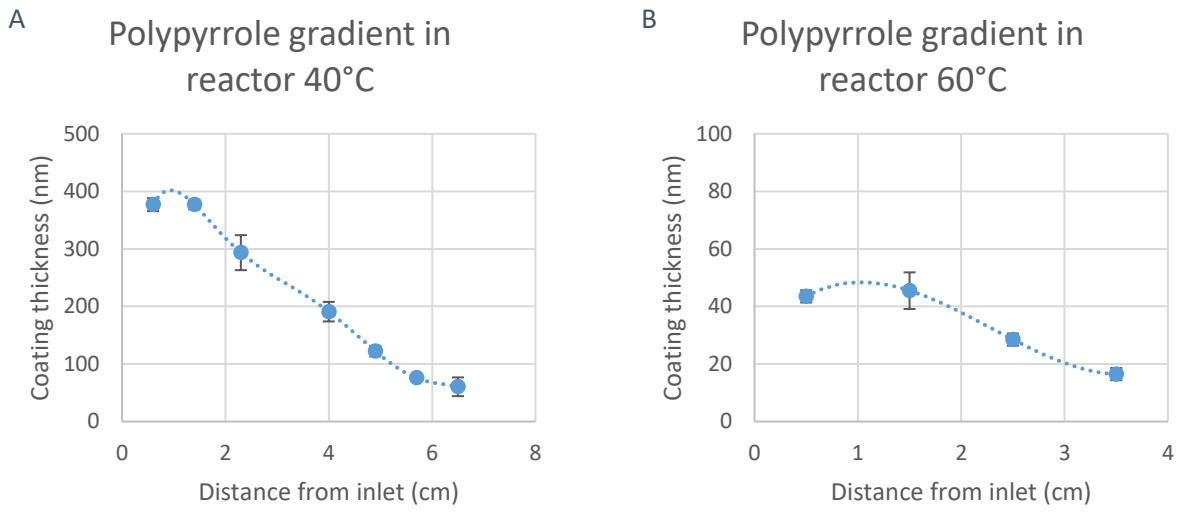

Figure 12: Coating thickness as a function of distance from the reactant inlet for the oCVD experiments at A) 40°C and B) 60°C. The coating thickness of the reaction at 50°C could not be determined because it was too small to measure with accuracy.

A deposition gradient is present at both reaction temperatures, with a decrease of coating thickness when moving further away from the inlet. For the purpose of this research, it is assumed that the same gradient is present on the TPU substrate. Therefore, the PPy coating thickness on the TPU substrates is estimated by interpolating the values from figure 12 (Table 5).

Still, it must be mentioned that it is challenging to assign a coating thickness when measuring in the range of 50 nm as the effect of surface morphology becomes more present at this stage.[45] On top of this, the difference in coating thickness for the reaction at 60°C is relatively low (Figure 12B). Therefore, these samples are critically regarded when measuring the effect of coating thickness on electromechanical behaviour.

Table 5: Coated TPU samples from different oCVD experiments, including the distance from the inlet and the calculated coating thickness. As the coating thickness of the reaction at 50°C could not be measured, it is assumed that the actual thickness is below the minimal measured value at 60°C (17nm).

Experiment	Temperature (°C)	Reaction time (min)	Sample name	Distance from the inlet (cm)	Coating thickness (nm)
Temperature 1	40	30	T40PPyL	0,49	355
			T40PPyM	3,49	223
			T40PPyS	6,49	63
Temperature 2	50	30	T50PPyL	1,69	<17
			T50PPyM	2,69	<17
			T50PPyS	3,69	<17
Temperature 3	60	40	T60PPyL	1,69	43
			T60PPyM	2,69	25
			T60PPyS	3,69	17

The coated TPU samples were tested on the tensile test to measure the effect of the PPy on the mechanical behaviour (stress-strain graphs are presented in appendix 3). The stress at 20% and 100% strain and the elastic modulus are calculated and compared the values of TPU (Figure 13). The graph shows that the coated TPU substrates do not significantly change their mechanical behaviour. This observation contradicts the results of the DMA tests, which suggested that PPy coating compromised the elasticity of the sample. However, the tensile tests are less precise, and the coated substrates were only tested three times compared to the TPU substrates that were tested ten times.

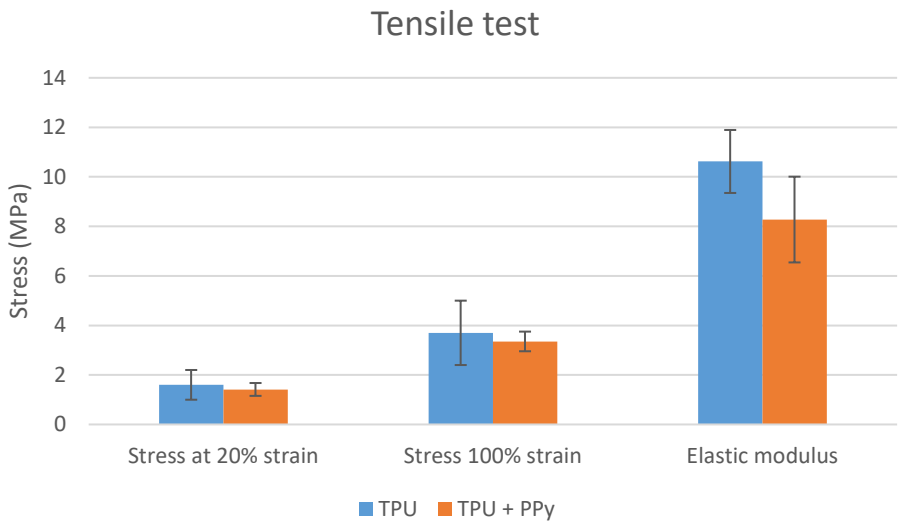

Figure 13: Tensile test of TPU and TPU coated with PPy (reaction time: 60 minutes, temperature: 40°C). T-test Stress at 20% strain (P=0.11), Stress at 100% strain (P=0.08), Elastic modulus (P=0.13)

4.3 ELECTROMECHANICAL BEHAVIOUR

4.3.1 Conductivity

The effect of coating thickness on the conductivity is demonstrated in graph 14A. The graph shows that the reactions at 40°C synthesise an SC where a higher coating thickness results in lower conductivity. This relation was also found in a study on PEDOT films by Ugur et al..[37] Their research proposed that the charge carrier mechanism changes from 2D to 3D when the coating thickness increases. This is because 2D structures have a more aligned structure, while 3D structures have a more disorderly network. [29] This proposition is supported by the "Variable range hopping" models of Mott and Efros-Shklovskii and the empirical results that were compared to these models.[37] The reaction at 60°C did not support this relation. However, in this experiment, the samples had a similar coating thickness which was relatively low. Hence, a less significant influence of coating thickness on electrical behaviour can be expected.

The difference of graphs 14A and 14B conclude that higher temperatures have a negative effect on conductivity. The conductivity values of the experiment at 40°C vary from 29 to 82 S/cm, which are comparable values relative to other research with conductive coatings.[46] At 60°C, though, the values range from 0.2 to 2.3 S/cm. Coming back to the hypothesis, it was expected that higher temperatures would promote the diffusion of PPy in the TPU structure. However, at higher temperatures, the vapour pressure increases, which limits surface absorption. This could have been the reason that the PPy adsorption on and into the TPU substrate was limited.

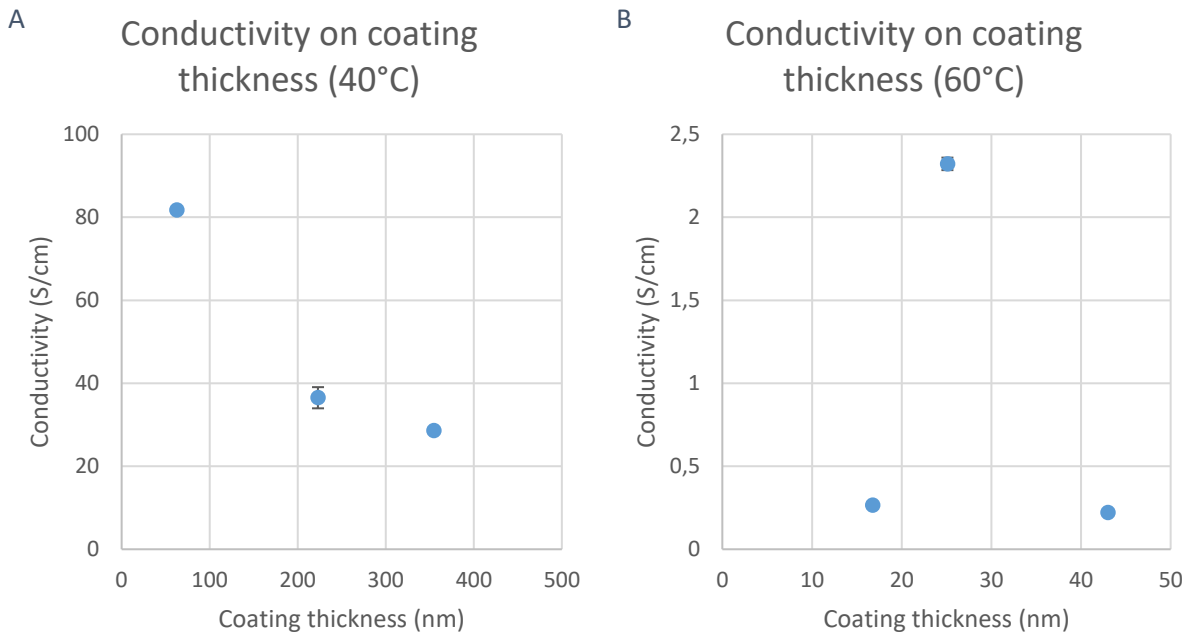

Figure 14: Conductivity of PPy coated TPU samples at a different coating thickness for reaction at A) 40°C and B) 60°C. As the coating thickness could not be measured for the experiment at 50°C, the conductivity could not be calculated for these samples.

4.3.2 Piezoresistivity

The PPy coated TPU samples were tested on the change in resistance when put under deformation, also called piezoresistivity. As a general trend, all PPy coated TPU samples lose conductivity under deformation, meaning that, under strain, the conductive pathway through the material is broken down, resulting in an increased electrical resistance (Figure 15). This behaviour was also noticed by Sarkar et al. In their research, in situ optical microscopy was used to determine the cracks of a PEDOT: PSS coating on a PDMS substrate when under strain. They concluded that the conductivity change is proportional to the amount and size of cracks on the conductive coating formed perpendicular to the strain direction.[47] This formation of cracks perpendicular to the strain direction was also spotted on the samples in this research (Figure 16).

Regarding the samples from the reaction at 40°C, the graph shows a relation between coating thickness and piezoresistive behaviour (Figure 15A). Here, the SC with the thickest coating shows a relatively fast increase of resistance when put under strain, while thinner coatings tend to show a more controlled linear increase of resistance with respect to strain. This behaviour can be explained by the effect of thickness on the macrostructure of PPy. Wang et al. studied the mechanical properties of polymer conductive coatings and the factors influencing them.[48] They reported that larger coating layers readily have microscopic defects in the structure, which causes early fracturing by applied stress. This corroborates with the findings in the piezoresistivity graph (figure 15A) and the local fracturing of the PPy layer (Figure 16A).

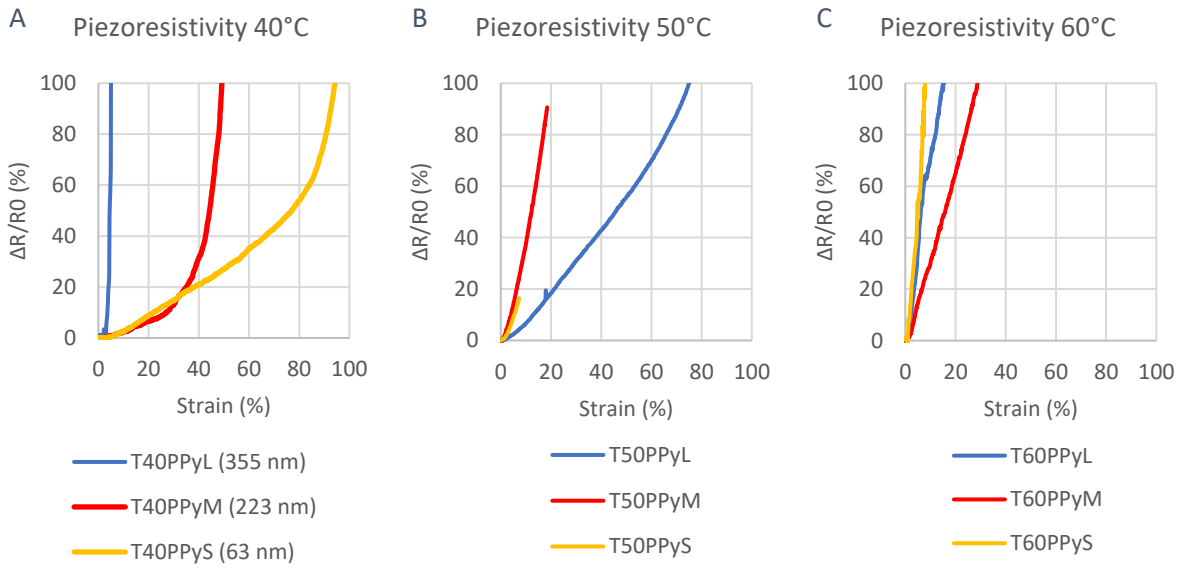

Figure 15: Piezoresistivity tests of PPy coated TPU samples with different coating thicknesses and reaction temperatures. The sudden end of the graph indicates the transition from conductive to completely insulating behaviour

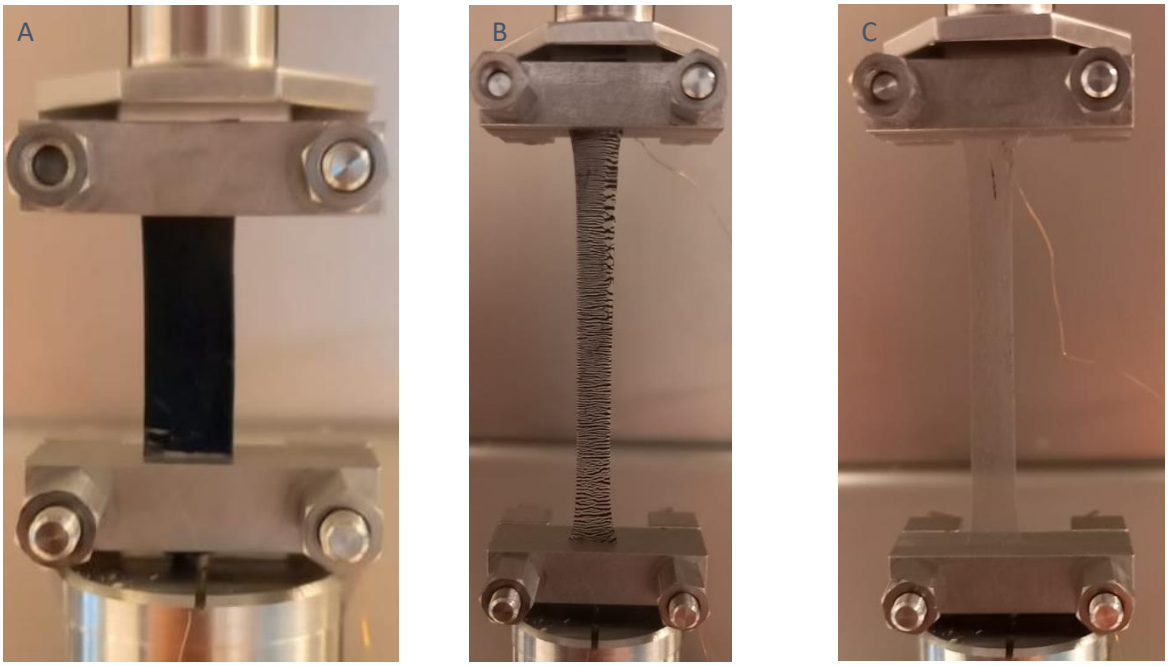

Figure 16: PPy fragmentation of A) T40PPYL, B) T40PpyM, and C) T40PPyS. The picture was taken at the point of becoming completely insulating.

The piezoresistive tests have shown that all PPy coated TPU substrates lose conductivity when being subjected to strain. This behaviour is found in other research where the focus lies on synthesising a piezoresistive sensor.[49–53] In the piezoresistive strain sensors application, the gauge factor is a commonly used value representing the ratio of change in resistance and strain. The gauge factor is calculated for all samples by taking the slopes of the linear region of the graphs (Table 6). The samples from higher temperatures generally have a higher gauge factor, indicating a more substantial response of resistance under deformation. This suggests that these samples have a conductive network which is more easily broken down under deformation.

Table 6: Gauge factors calculated from the piezoresistivity graphs. The gauge factor of T40PPyL could not be calculated as there was no constant increase in resistance

Sample name	Gauge factor
T40PPyL	-
T40PPyM	0,26
T40PPyS	0,50
T50PPyL	0,88
T50PPyM	3,36
T50PPyS	1,37
T60PPyL	4,55
T60PPyM	2,76
T60PPyS	7,32

Among the tested samples, T40PPyS and T50PPyL showed piezoresistive behaviour within respectable ranges of relative resistance (0.5 and 0.8) and strain (75% and 70%). Therefore, these two samples are further tested on durability.

4.3.3 Durability

In the following tests, the change in resistance is measured after multiple stretching cycles. When deciding the repetitive strain value, two restraints were of importance. On one side, the signal should be large enough to see the change in resistance, and on the other side, the material should not irreversibly deform. When designing the durability method, the samples did not show resistance change with cycles of 10% strain and lower. A possible reason for this could be that cracks occurred only after a certain amount of strain. This behaviour was also found on the PEDOT/PSS coated PDMS substrates in the research of Sarkar et. Al. As noted in the previous section, they found the relation between microcrack formation and resistance increase. What they also found is a delay of resistance at low strain values. They suggested that the change in resistance is dominated by wrinkles of the coating instead of cracks within the lowest strain range. These wrinkles can stretch without suffering from an inferior charge carrier mechanism.[47] As this behaviour was also observed in the durability tests, the strain was increased to 15%. The elastic region of the selected TPU was determined at 20% strain (Figure 8). Therefore, the stretching cycles were set to 15% strain to ensure the stretchable material did not deform.

Both samples share the same behaviour (figure 17). The first cycle causes the most significant increase of resistance which is barely coming down again. In the consecutive cycles, the resistance is partially recovered but keeps increasing, which means that the conductivity cannot fully restore after deformation. Furthermore, the graphs indicate that T50PPyL loses significantly more conductivity after each cycle compared to the sample of T40PPyS. This observation correlates with the piezoresistivity tests (Figure 15), where the increase of resistance under strain was twice as much for T50PPyL compared to T40PPyS. As a general trend, the durability test shows that both samples are not yet suitable to function as a piezoresistive sensor as they do not recover the conductivity after multiple stretching cycles.

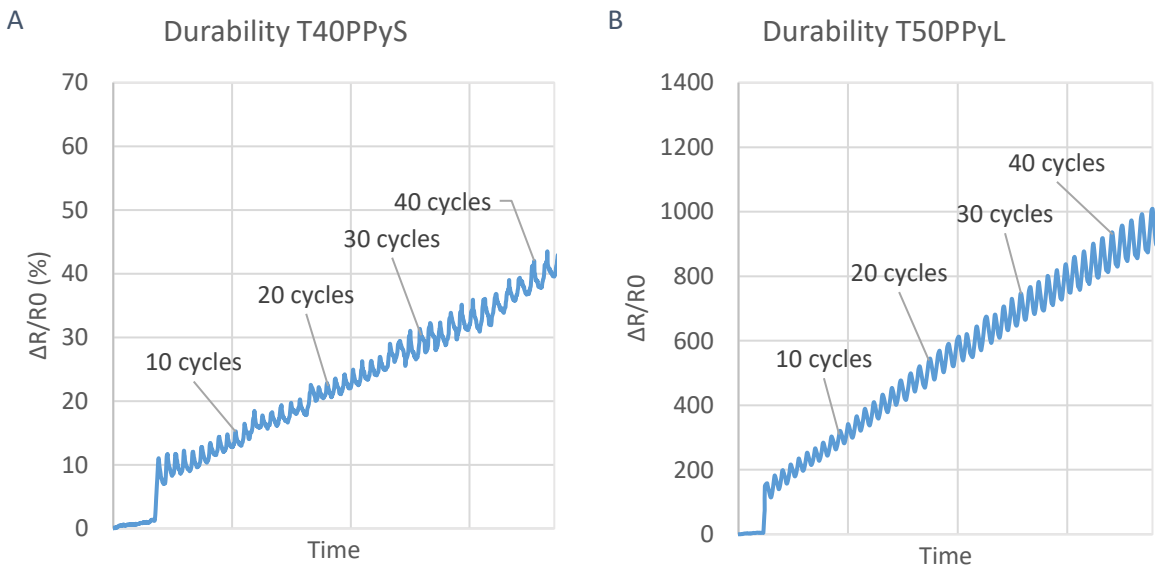

Figure 17: Change of resistance of samples A) T40PPys and B) T50PPyL after multiple stretching cycles of 15% strain. The actual test went over to 100 cycles. However, shortly after 50 cycles, the material approached insulating behaviour.

To compare the change of resistance with mechanical behaviour, the load strain graph is obtained of cycles 1, 10, 20, 30 and 40 (Figure 18). The graphs show that both samples have deformed irreversibly after the first cycle, explaining the significant resistance increase in figure 17. However, in consecutive cycles, the material does not show irreversible deformation, suggesting that the deformation of the substrate did not completely cause the limited durability observed in graph 17.

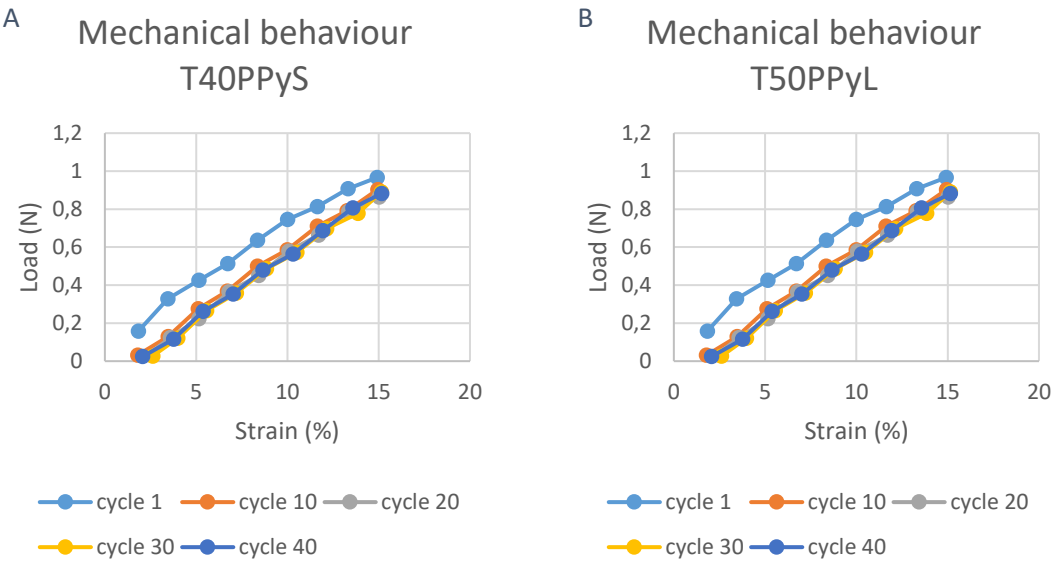

Figure 18: Mechanical behaviour of sample A) T40PPyS and B) T50PPyL during durability tests

To summarise, this thesis included the synthesis of a PPy/TPU based SC with heterogeneous assembly design using oCVD with the overarching objective to explore the potential of oCVD in the synthesis of stretchable conductors. The SC with the best performance was retrieved from the reaction at 40°C and had a coating thickness of 63 nm. While the durability test showed that the conductivity was not recovered after multiple stretching cycles, it had a respectable conductivity of 82 S/cm, and when strained to 75%, it showed a linear increase of resistance up to 50%. For comparison, the performance of this sensor is compared to other recently reported sensors (Table 7). From these reports, the sensors have in common that they can retrieve conductivity after multiple stretching cycles, probably due to the higher elasticity of the substrates. Nevertheless, the SC reported in this research could be of interest in piezoresistive sensor applications, provided that the durability improves.

Table 7: Previously reported PPy-based strain sensors

Substrate	Method	Strain range (%)	Resistance range (%)	Reference
Porous TPU	In situ polymerization	0-50	0-116	[49]
Silicone Rubber	Drop casting	0-100	0-120	[50]
Polyvinylpyrrolidone/PDMS (electrospun)	Vapour phase polymerization	0-50	0-80	[51]
Cotton	In situ polymerization	0-35	0-45	[52]
Polyester/Spandex	In situ polymerization	0-71	0-30	[53]

5 CONCLUSION

This work comprises the synthesis, analysis and performance of a PPy/TPU based SC using oCVD. Based on the tensile test and cyclic loading test, the Elastolan 1170 A10 was most suitable for an SC because of its low stiffness and good elasticity (20% strain). Therefore, this selected type of TPU was coated with PPy using oCVD. In three experiments, the coating thickness and reaction temperature (40°C, 50°C, 60 °C) were varied, after which the coated samples were characterised and analysed on electromechanical behaviour.

The FTIR scan indicated the C=C, C-N, C-H, and C-C bonds meaning that the PPy deposited successfully on the substrates. DSC and DMA measured a higher T_g of the PPy coated samples, indicating the reduced mobility of the polymer chains and demonstrated the intramolecular interaction between PPy and TPU. DMA also showed a decreased tan delta and storage modulus for the coated TPU substrate, implying that the PPy coating compromises the elasticity of the composite. Tensile tests, however, demonstrated that the PPy coating did not influence the stress-strain behaviour of the TPU substrates. Profilometry showed that the deposition rate was dependent on both location in the reactor as substrate temperature. The latter showed a negative temperature effect on the deposition rate, suggesting that the deposition mechanism is rather mass transfer limited than kinetically limited at the used temperatures.

The PPy coated TPU substates reached a conductivity as high as 82 S/cm. The samples with thicker coatings tended to have a decreased conductivity, which is likely caused by the less aligned PPy structure. At higher temperatures, very thin coatings were produced. However, this had an adverse effect resulting in a low conductivity. The piezoresistivity tests revealed that resistance increased under strain, caused by cracks on the PPy coating. In particular, samples with thicker PPy coatings tended to endure local fragmentation of the coating when put under strain and, as a result, become electrically insulating under a minimal amount of strain. On the other side, the thinner coatings showed a linear increase of resistance in a 0-75% strain range. The samples from higher reaction temperatures showed a relatively fast increase of resistance under strain. The durability test showed that samples from a lower temperature lost less conductivity after multiple cycles. However, no samples were able to recover their conductivity completely. Concluding, the SC with the best electromechanical performance was retrieved from the reaction at 40°C and had a coating thickness of 63nm. While it showed a sufficient electromechanical performance, the durability should improve. Therefore, more research is required for this SC to be of interest for applications in piezoresistive strain sensors.

6 RECOMMENDATIONS

6.1 PRODUCT RECOMMENDATIONS

The tests on electromechanical behaviour showed that these PPy coated TPU samples could not fully recover deformation after stretching. To make this composite more suitable for applications in stretchable electronics, it should have increased durability. The currently used Elastolan 1170 A10 had an elastic region until 20%. However, when coated with PPy, the elasticity may be decreasing. Therefore it is recommended to select a new substrate or modify the current substrate to increase elasticity. Increasing the elasticity of the material could be done by changing the macrostructure by, for example by electrospinning.[54]

The macrostructure could also be changed into a porous network. For example, in other research by Li et al., PPy based strain sensors were made by in situ polymerisations inside and on a porous PU substrate. SEM images showed interpenetration at the interface of the two layers, making the two components strongly anchored.[49] The diffusion of PPy into a porous substrate could also work for oCVD and possibly increase the electromechanical behaviour by improving the support of the TPU to the PPy structure.

The piezoresistive tests demonstrated the possible interest of application in strain sensors. To further explore the potential of this material, more tests are required. As the structure of the PPy influences the electromechanical behaviour, the samples should be analysed by SEM.[47] This can visualise how PPy is coated on and into the TPU structure. Furthermore, when applying SEM in-situ while testing piezoresistivity, the effect of PPy structure on electromechanical behaviour can be visualised. Another recommended test is the response time which is used in sensor applications to test whether the change in resistance to deformation is adequate.[50] This test could give a more detailed insight into the electrical response at small deformations.

6.2 PROCESS RECOMMENDATIONS

In oCVD, all essential process parameters must be stable to control the layer growth. While temperature and pressure are regulated in the reactor, the reactant flow is not. As shown in the experimental section, the reactant flows are calibrated before and after the reaction. It was found that reactant flows changed during the reaction, meaning that the reactant flow rate was unstable. Therefore, it is recommended to install continuous mass flow measurement in the reactant lines to increase the reproducibility of the experiments

During the oCVD experiment, the reactant lines became clogged over time, influencing the distribution of chemicals in the reaction chamber. The possible cause for the clogging could be the sudden temperature decrease from 110°C in the lines to 40°C in the reaction chamber. This research found that a higher substrate temperature results in less adsorption on the substrates. Therefore a new experimental setup is recommended where the reaction chamber is kept at elevated temperatures, and the substrates are placed on a chiller. This way, the deposition only occurs on the substrate and not at other locations in the reactor.

As the coating thickness is still dependent on the location of the substrate in the oCVD reactor, it is challenging to determine the coating thickness with accuracy. Therefore, it is recommended to research the deposition gradient measured by profilometry at multiple locations in the reactor.

7 REFERENCES

1. Cheng T, Zhang Y, Lai WY, Huang W. Stretchable thin-film electrodes for flexible electronics with high deformability and stretchability. *Adv Mater*. 2015;27(22):3349-3376. doi:10.1002/adma.201405864

2. Wu W. Stretchable electronics: functional materials, fabrication strategies and applications. *Sci Technol Adv Mater*. 2019;20(1):187-224. doi:10.1080/14686996.2018.1549460

3. Liu Y, Pharr M, Salvatore GA. Lab-on-Skin: A Review of Flexible and Stretchable Electronics for Wearable Health Monitoring. *ACS Nano*. 2017;11(10):9614-9635. doi:10.1021/acsnano.7b04898

4. O'Regan T, Perconti P. Energy-efficient and flexible electronics for military applications. *SPIENewsroom*. Published online 2015. doi:10.1117/2.1201503.005820

5. Almuslem AS, Shaikh SF, Hussain MM. Flexible and Stretchable Electronics for Harsh-Environmental Applications. *Adv Mater Technol*. 2019;4(9):1-18. doi:10.1002/admt.201900145

6. Wu H, Huang YA, Xu F, Duan Y, Yin Z. Energy Harvesters for Wearable and Stretchable Electronics: From Flexibility to Stretchability. *Adv Mater*. 2016;28(45):9881-9919. doi:10.1002/adma.201602251

7. Ratha S, Kumar Samantara A. *Supercapacitor: Instrumentation, Measurement and Performance Evaluation Techniques*.; 2018. doi:10.1007/978-981-13-3086-5

8. Kim DC, Shim HJ, Lee W, Koo JH, Kim DH. Material-Based Approaches for the Fabrication of Stretchable Electronics. *Adv Mater*. 2020;32(15):1-29. doi:10.1002/adma.201902743

9. Noh JS. Conductive elastomers for stretchable electronics, sensors and energy harvesters. *Polymers (Basel)*. 2016;8(4). doi:10.3390/polym8040123

10. Thomas S, Janusz D, Haponiuk J, Reghunadhan A. *Polyurethane Polymers: Blends and Interpenetrating Polymer Networks*.; 2017.

11. Sonnenschein MF. *Polyurethanes: Science, Technology, Markets, and Trends*.; 2014.

12. Squiller E, Danielmeier K, Kruppa P. *Polyurethanes: Coatings, Adhesives and Sealants*.; 2019. doi:10.1515/9783748600473

13. Zhao Y, Kim A, Wan G, Tee BCK. Design and applications of stretchable and self-healable conductors for soft electronics. *Nano Converg*. 2019;6(1). doi:10.1186/s40580-019-0195-0

14. Anzar N, Hasan R, Tyagi M, Yadav N, Narang J. Carbon nanotube - A review on Synthesis, Properties and plethora of applications in the field of biomedical science. *Sensors Int*. 2020;1(February):100003. doi:10.1016/j.sintl.2020.100003

15. Sekitani T, Noguchi Y, Hata K, Fukushima T, Aida T, Someya T. A rubberlike stretchable active matrix using elastic conductors. *Science (80-)*. 2008;321(5895):1468-1472. doi:10.1126/science.1160309

16. Wang P, Peng Z, Li M, Wang YH. Stretchable Transparent Conductive Films from Long Carbon Nanotube Metals. *Small*. 2018;14(38). doi:10.1002/smll.201802625

17. Peng H, LI Q, Chen T. *Industrial Applications of Carbon Nanotubes*. 1st editio.; 2016.

18. Lee P, Lee J, Lee H, et al. Highly stretchable and highly conductive metal electrode by very

long metal nanowire percolation network. *Adv Mater*. 2012;24(25):3326-3332. doi:10.1002/adma.201200359

19. Namsheer K, Rout CS. Conducting polymers: a comprehensive review on recent advances in synthesis, properties and applications. *RSC Adv*. 2021;11(10):5659-5697. doi:10.1039/d0ra07800j

20. Kayser L V., Lipomi DJ. Stretchable Conductive Polymers and Composites Based on PEDOT and PEDOT:PSS. *Adv Mater*. 2019;31(10):1-13. doi:10.1002/adma.201806133

21. Sadasivuni K, Cabibihan J-J, Ponnamma D, AlMaadeed MA, Kim J. *Biopolymer Composites in Electronics*.; 2016.

22. Jones RA, Bean GP. The Chemistry of Pyrroles. *Org Chem A Ser Monogr*. 1977;Vol. 34:538.

23. Camurlu P. Polypyrrole derivatives for electrochromic applications. *RSC Adv*. 2014;4(99):55832-55845. doi:10.1039/c4ra11827h

24. Clayden J, Greeves N, Warren S. *Organic Chemistry*.; 2012.

25. Shi L, Liu J, Wang Y, Gao B, Sillanpää M. Organic photoelectrocatalytic filtration membrane originated from PEDOT modified PVDF. *Chem Eng J*. 2021;405(September 2020):126954. doi:10.1016/j.cej.2020.126954

26. Zhao JIE. *Solution-Processable Conductive Graphene-Based Materials for Flexible Electronics*.; 2019.

27. Trung TQ, Lee NE. Recent Progress on Stretchable Electronic Devices with Intrinsically Stretchable Components. *Adv Mater*. 2017;29(3). doi:10.1002/adma.201603167

28. Baxamusa SH, Im SG, Gleason KK. Initiated and oxidative chemical vapor deposition: A scalable method for conformal and functional polymer films on real substrates. *Phys Chem Chem Phys*. 2009;11(26):5227-5240. doi:10.1039/b900455f

29. Heydari Gharahcheshmeh M, Gleason KK. Device Fabrication Based on Oxidative Chemical Vapor Deposition (oCVD) Synthesis of Conducting Polymers and Related Conjugated Organic Materials. *Adv Mater Interfaces*. 2019;6(1):1-27. doi:10.1002/admi.201801564

30. Ashurbekova K, Ashurbekova K, Botta G, Yurkevich O, Knez M. Vapor phase processing : a novel approach for fabricating functional. Published online 2020.

31. Wang M, Kovacik P, Gleason KK. Chemical Vapor Deposition of Thin, Conductive, and Fouling-Resistant Polymeric Films. *Langmuir*. 2017;33(40):10623-10631. doi:10.1021/acs.langmuir.7b02646

32. Drewelow G, Wook Song H, Jiang ZT, Lee S. Factors controlling conductivity of PEDOT deposited using oxidative chemical vapor deposition. *Appl Surf Sci*. 2020;501(October 2019):144105. doi:10.1016/j.apsusc.2019.144105

33. Smolin YY, Soroush M, Lau KKS. Oxidative chemical vapor deposition of polyaniline thin films. *Beilstein J Nanotechnol*. 2017;8(1):1266-1276. doi:10.3762/bjnano.8.128

34. Howden RM, McVay ED, Gleason KK. OCVD poly(3,4-ethylenedioxythiophene) conductivity and lifetime enhancement via acid rinse dopant exchange. *J Mater Chem A*. 2013;1(4):1334-1340. doi:10.1039/c2ta00321j

35. Heydari Gharahcheshmeh M, Gleason K. Using volatile liquid oxidant in PEDOT synthesis by oxidative Chemical Vapor Deposition (oCVD). Published online 2019.

36. Yin L, Lv J, Wang J. Structural Innovations in Printed, Flexible, and Stretchable Electronics. *Adv Mater Technol*. 2020;5(11):1-18. doi:10.1002/admt.202000694

37. Ugur A, Katmis F, Li M, et al. Low-Dimensional Conduction Mechanisms in Highly Conductive and Transparent Conjugated Polymers. *Adv Mater*. 2015;27(31):4604-4610. doi:10.1002/adma.201502340

38. Matsunaga K, Sato K, Tajima M, Yoshida Y. Gas permeability of thermoplastic polyurethane elastomers. *Polym J*. 2005;37(6):413-417. doi:10.1295/polymj.37.413

39. Kalnins D. Preparation of conductive coatins. Solution modification and CVD furnished coatings. Published online 2019.

40. Kaviani S, Mohammadi Ghaleni M, Tavakoli E, Nejati S. Electroactive and Conformal Coatings of Oxidative Chemical Vapor Deposition Polymers for Oxygen Electroreduction. *ACS Appl Polym Mater*. 2019;1(3):552-560. doi:10.1021/acsapm.8b00240

41. Fu Y, Su Y, Manthiram A. Sulfur-Polypyrrole Composite Cathodes for Lithium-Sulfur Batteries Sulfur-Polypyrrole Composite Cathodes for Lithium-Sulfur Batteries. 2016;(June 2012). doi:10.1039/C2RA20393F

42. Yanilmaz M, Kalaoglu F, Karakas H, Sarac AS. Preparation and Characterization of Electrospun Polyurethane – Polypyrrole Nanofibers and Films. 2010;(February 2016). doi:10.1002/app.36386

43. Menard KP, Menard NR. *Dynamic Mechanical Analysis: Third Edition*.; 2020.

44. Balint R, Cassidy NJ, Cartmell SH. Conductive polymers: Towards a smart biomaterial for tissue engineering. *Acta Biomater*. 2014;10(6):2341-2353. doi:10.1016/j.actbio.2014.02.015

45. Kim DO, Lee PC, Kang SJ, et al. In-situ blends of polypyrrole/poly(3,4-ethylenedioxythiopene) using vapor phase polymerization technique. *Thin Solid Films*. 2009;517(14):4156-4160. doi:10.1016/j.tsf.2009.02.028

46. Wang M, Wang X, Moni P, et al. PROGRESS REPORT CVD Polymers for Devices and Device Fabrication. 2017;1604606. doi:10.1002/adma.201604606

47. Sarkar B, Satapathy DK, Jaiswal M. Soft Matter Wrinkle and crack-dependent charge transport in a uniaxially strained conducting polymer film on a flexible substrate †. Published online 2017:5437-5444. doi:10.1039/c7sm00972k

48. Wang XS, Tang HP, Li XD, Hua X. Investigations on the mechanical properties of conducting polymer coating-substrate structures and their influencing factors. *Int J Mol Sci*. 2009;10(12):5257-5284. doi:10.3390/ijms10125257

49. Li M, Li H, Zhong W, Zhao Q, Wang D. Stretchable conductive polypyrrole/polyurethane (PPy/PU) strain sensor with netlike microcracks for human breath detection. *ACS Appl Mater Interfaces*. 2014;6(2):1313-1319. doi:10.1021/am4053305

50. Kurian AS, Souri H, Mohan VB, Bhattacharyya D. Highly stretchable strain sensors based on polypyrrole-silicone rubber composites for human motion detection. *Sensors Actuators, A Phys*. 2020;312:112131. doi:10.1016/j.sna.2020.112131

51. Niu H, Zhou H, Wang H, Lin T. Polypyrrole-Coated PDMS Fibrous Membrane: Flexible Strain Sensor with Distinctive Resistance Responses at Different Strain Ranges. *Macromol Mater Eng*. 2016;301(6):707-713. doi:10.1002/mame.201500447

52. Hao D, Xu B, Cai Z. Polypyrrole coated knitted fabric for robust wearable sensor and heater. *J Mater Sci Mater Electron*. 2018;29(11):9218-9226. doi:10.1007/s10854-018-8950-2

53. Chen X, Li B, Qiao Y, Lu Z. Preparing polypyrrole-coated stretchable textile via low-temperature interfacial polymerization for highly sensitive strain sensor. *Micromachines*. 2019;10(11). doi:10.3390/mi10110788

54. Pedicini A, Farris RJ. Mechanical behavior of electrospun polyurethane. *Polymer (Guildf)*. 2003;44(22):6857-6862. doi:10.1016/j.polymer.2003.08.040

8 APPENDIX

1. Tensile tests on Neorez series.

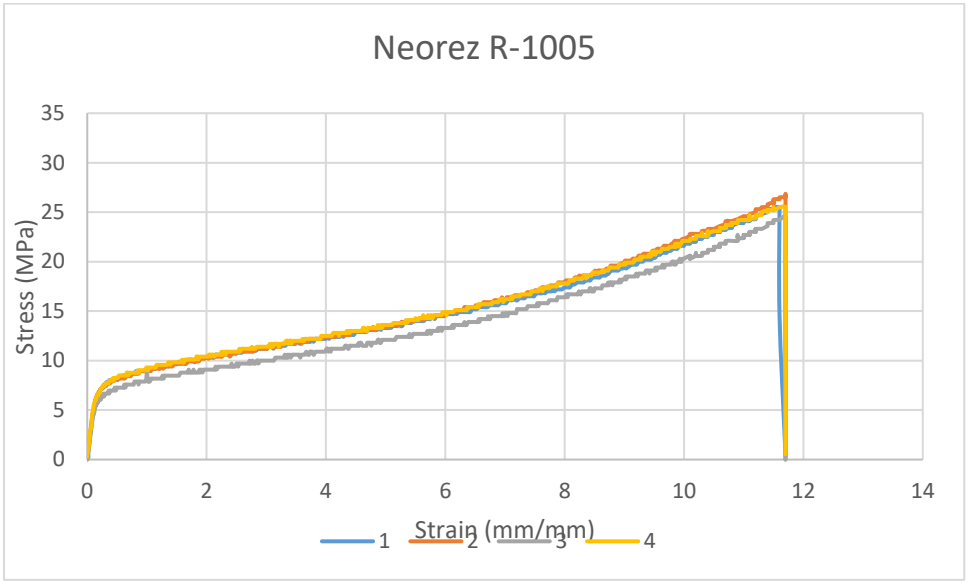

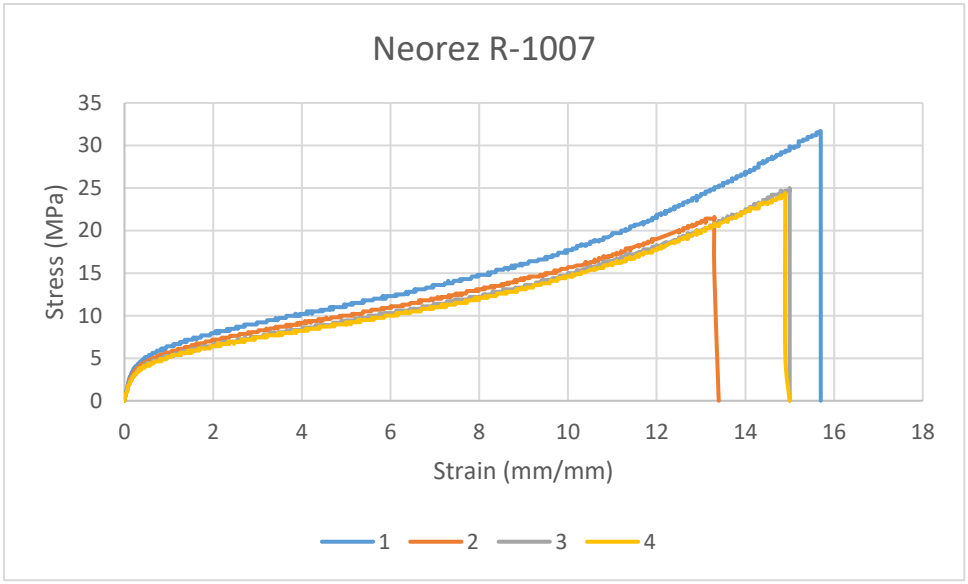

2. Tensile test on Elastolan series.

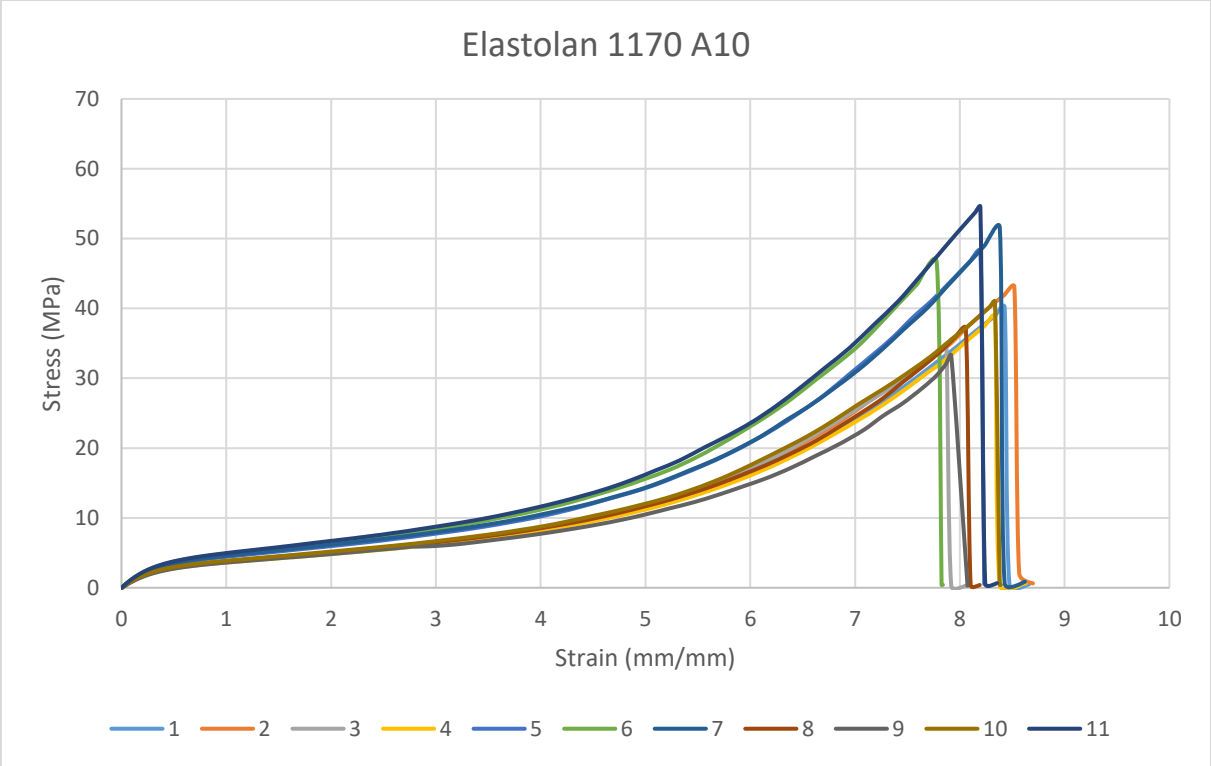

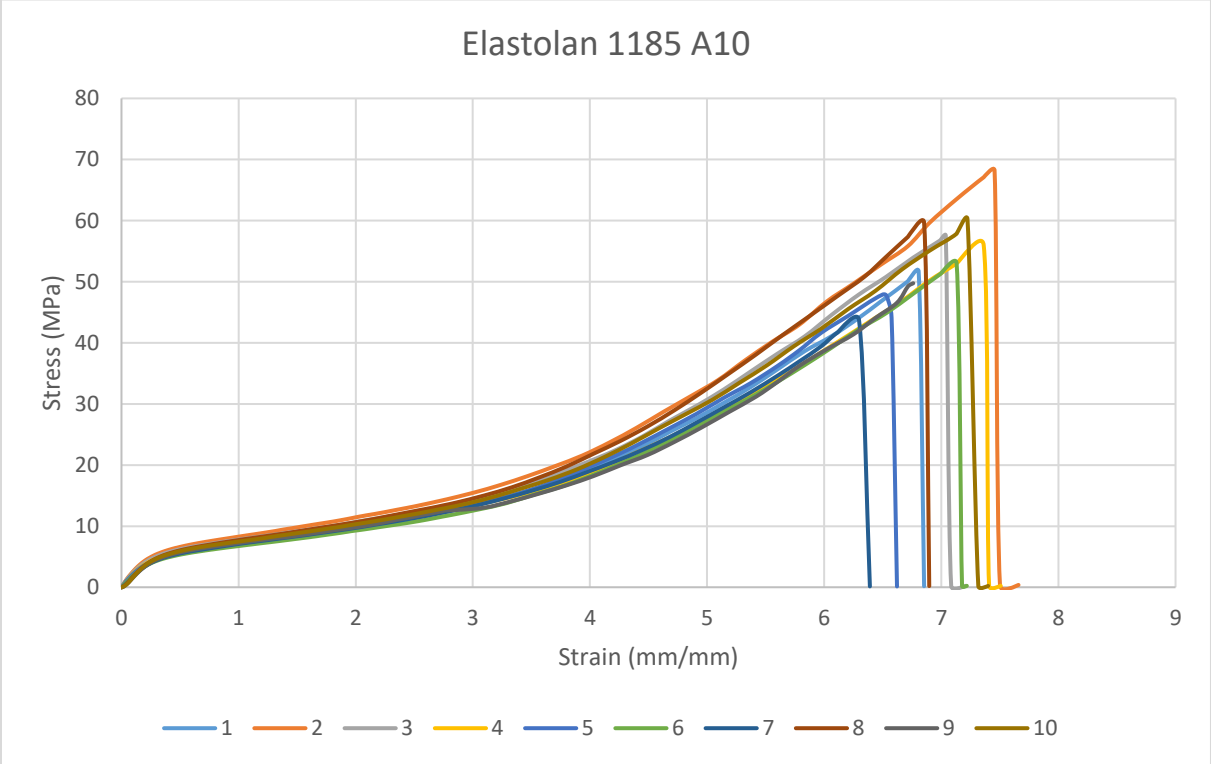

3. Tensile test on PPy coated elastolan 1170 A10